European Journal of Radiology 118 (2019) 277–284

Contents lists available at ScienceDirect

European Journal of Radiology

journal homepage: www.elsevier.com/locate/ejrad

Research article

Accelerating anatomical 2D turbo spin echo imaging of the ankle using compressed sensing

Alexandra S. Gersing[a,b,*], Jannis Bodden[a], Jan Neumann[a], Maximillian N. Diefenbach[a], Sophia Kronthaler[a], Daniela Pfeiffer[a], Carolin Knebel[c], Thomas Baum[e], Benedikt J. Schwaiger[a], Andreas Hock[d], Ernst J. Rummeny[a], Klaus Woertler[a], Dimitrios C. Karampinos[a]

[a] Department of Radiology, Technical University of Munich, Ismaninger Strasse 22, 81675, Munich, Germany
[b] Department of Radiology and Biomedical Imaging, University of California, 185 Berry Street, Suite 350, San Francisco, CA, 94107, USA
[c] Department of Orthopaedic Surgery, Klinikum rechts der Isar, Technical University of Munich, Munich, Germany
[d] Philips MR Clinical Science, Zurich, Switzerland
[e] Department of Neuroradiology, Technical University of Munich, Ismaninger Strasse 22, 81675 Munich, Germany

ARTICLE INFO

Keywords:
Magnetic resonance imaging
Musculoskeletal system
Diagnostic imaging
Accelerated data acquisition
Sparse sampling

ABSTRACT

Introduction: To assess the feasibility and diagnostic value of compressed sensing for accelerating two-dimensional turbo spin echo imaging of the ankle.

Materials and methods: Ankles of 20 volunteers were scanned (mean age 30.2 ± 7.3 years, 13 men) at 3 T MRI. Coronal and sagittal intermediate-weighted (IM) sequences with fat saturation as well as axial T2- and coronal T1-weighted sequences were acquired using parallel imaging based on sensitivity encoding (SENSE) only as well as with a combination of compressed sensing (CS) and SENSE. Compressed sensing is a technique that acquires less data through k-space random undersampling and enables a reduction in total acquisition time by 20%. All images were reviewed by two radiologists, image quality was graded using a 5-point Likert scale and signal-to-noise ratio (SNR) and contrast-to-noise ratio (CNR) of different anatomical structures of the ankle were assessed and compared between sequences with SENSE only and with the combination of CS and SENSE using Wilcoxon signed-rank tests and Cohen's kappa.

Results: There was a substantial to perfect agreement for the rating between the images acquired with SENSE only and with the combination of CS and SENSE when assessing cartilage, subchondral bone and ligaments (κ = 0.75 - 0.89). SNR was slightly higher for the combination of CS and SENSE sequences compared to the sequences acquired with SENSE only, yet this finding was not significant (P = 0.18-0.62). Moreover, CNR of cartilage/fluid, subchondral bone/cartilage, ligaments/fluid and ligaments/fat did not show significant differences between the sequences acquired with SENSE only and the combination of CS and SENSE ($P > 0.05$). The interreader agreement was substantial to excellent for both techniques (κ = 0.75 - 0.89).

Conclusions: Compressed sensing reduced the acquisition time of conventional MR imaging of the ankle by 20% without decreasing diagnostic image quality, SNR and CNR.

1. Introduction

The ankle is a complex joint with several oblique oriented ligaments and tendons [1–3]. Therefore, conventional 2D turbo spin echo (TSE) MR sequences need to be acquired in all three dimensions with a standard musculoskeletal magnetic resonance imaging protocol. Consequently, the standard musculoskeletal MR imaging protocol is associated with long examination times. The high resolution of such sequences is especially needed in order to depict the different anatomical structures and pathologies. High-resolution 2D TSE sequences are currently still limited by their long acquisition times.

Scan time can be reduced in general by using parallel imaging with a consequent decrease of the signal-to-noise ratio [4]. Scan time can be also reduced by performing sequences at lower resolution and longer

* Corresponding author.
E-mail addresses: alexandra.gersing@tum.de (A.S. Gersing), jannis.bodden@tum.de (J. Bodden), jan.neumann@tum.de (J. Neumann), maximilian.diefenbach@tum.de (M.N. Diefenbach), sophia.kronthaler@tum.de (S. Kronthaler), daniela.pfeiffer@tum.de (D. Pfeiffer), carolin.knebel@tum.de (C. Knebel), thomas.baum@tum.de (T. Baum), benedikt.schwaiger@tum.de (B.J. Schwaiger), andreas.hock@philips.com (A. Hock), ernst.rummeny@tum.de (E.J. Rummeny), klaus.woertler@tum.de (K. Woertler), dimitrios.karampinos@tum.de (D.C. Karampinos).

https://doi.org/10.1016/j.ejrad.2019.06.006
Received 14 February 2019; Received in revised form 11 May 2019; Accepted 10 June 2019

echo train length, which however result in a decrease of image quality [5–7]. An MR imaging acceleration technique has recently been introduced in order to reduce the acquisition time based on undersampling of k-space data, labelled as compressed sensing [8]. Compressed sensing (CS) relies on the compressibility of MR images. Pseudo-randomization of undersampling patterns in k-space result in noise-like aliasing, which is removed by sparsity constraints in the reconstruction [8–10]. This technique has previously shown to be useful in vascular, cardiac and body imaging [11]. Nevertheless, the use of this technique has remained limited in 2D musculoskeletal imaging, although in this field high quality 2D imaging is needed in order to visualize even subtle pathologies of joint structures [11].

Therefore, the purpose of the present study was to evaluate the use of compressed sensing to accelerate imaging of the ankle. Therefore, conventional 2D MR images of ankles were acquired using sensitivity encoding (SENSE) parallel imaging as well as a combination of CS and SENSE in order to assess whether CS reduces the overall scan time while maintaining diagnostic image quality.

2. Materials and methods

2.1. Study subject selection

The study was approved by the institutional review board. All 20 volunteers gave their written informed consent and were recruited between April and August 2018. Of these, 17 volunteers reported no history of prior ankle pain, trauma or surgery. Three volunteers had a history of trauma within the last two years and one of these volunteers reported on persisting pain when performing weight bearing activities, yet, none of the volunteers had undergone surgery. Exclusion criteria for recruitment were the general exclusion criteria for MR imaging (pacemaker, other implanted electronic devices, pregnancy, etc).

2.2. Data acquisition

Imaging was performed on one 3 T MR scanner (Ingenia Elition; Philips Healthcare, Best, the Netherlands) using a dedicated 16-channel ankle coil (Medical Advances). In order to reduce motion artifacts, the ankle was fixated within the coil. Axial T2-weighted TSE sequences, coronal T1-weighted TSE sequences and coronal as well as sagittal intermediate-weighted (IM) TSE sequences with spectral presaturation with Inversion Recovery (SPIR) for fat saturation were obtained using SENSE alone as well as using a combination of CS and SENSE from one ankle in each volunteer. Further details of the employed imaging acquisition protocols are given in Table 1.

The combination of CS and SENSE is the technique used in the current study, and is also labelled as Compressed SENSE or C-SENSE. This combination of CS and SENSE uses the coil sensitivity information from a SENSE calibration scan randomly undersamples both the central and outer part of k-space, following a smooth sampling density as moving from the center to outer parts of k-space. The acquisition of the combination of CS and SENSE as well as the reconstruction were based on the vendor's implementation (Compressed SENSE, Philips Healthcare). A single CS acceleration factor was defined for each imaging sequence and the sampled k-space pattern (central and outer part) was defined based on the vendor's implementation. In order to maintain a balance between noise reduction and data consistency for CS, an iterative L1-minimization reconstruction technique, forcing data fidelity, and image sparsity in the wavelet domain was used.

Compared to previous studies evaluating CS methodologies for 3D imaging sequences in the knee [4], the present work focused on high in-plane resolution 2D imaging, in order to achieve the highest detection rate possible for pathologies of the ankle.

For assessment of the SNR, sagittal and coronal MR sequences were performed twice in 8 volunteers on the same ankle without repositioning between the repeated scans. In total, the 2D TSE protocol

Table 1
Sequence parameters of the sequences acquired using sensitivity encoding (SENSE) only and using a combination of compressed sensing (CS) and SENSE (CS + SENSE).

Acquired voxel size (mm)^3	0.33 × 0.38 × 2.5	0.33 × 0.38 × 2.5	0.25 × 0.39 × 2.5	0.25 × 0.39 × 2.5	0.2 × 0.3 × 2.5	0.2 × 0.3 × 2.5	0.15 × 0.28 × 2.0	0.15 × 0.28 × 2.0
Slice thickness (mm)	2.5	2.5	2.5	2.5	2.5	2.5	2.0	2.0
Matrix size (mm)	394 × 329	349 × 341	605 × 385	605 × 388	653 × 429	653 × 436	932 × 491	932 × 491
Echo Number	1	1	1	1	1	1	1	1
Echo Time (TE; ms)	50	50	50	50	18	18	70	70
Field of view (FOV; mm)^3	130	130	151	151	131	131	140	140
Number of slices	35	35	35	35	35	35	35	35
Repitition time (TR; ms)	2500-6000	2500-6000	2500-6000	2500-6000	450-850	450-850	shortest	shortest
Refocusing flip angle (°)	90	90	90	90	90	90	90	90
Bandwidth (Hz / Pixel)	305	305	158	158	240	240	189	189
Echo train length	7	7	7	7	6	6	19	19
Total accelera-tion factor	2	2.5	2	2.5	2	2.5	2	2.5
Acquisition time (min:sec)	4:14	3:26	3:54	3:26	5:27	4:20	6:10	4:31
	SENSE	CS + SENSE	SENSE	CS + SENSE	SENSE	CS + SENSE	SENSE	CS + SENSE
	PD/SPIR coronal		PD/SPIR sagittal		T1 coronal		T2 axial	

with the combination of CS and SENSE (total scan duration 15 min 47 s) was 20.1% shorter than the same 2D TSE scan protocol of the ankle performed with SENSE only (total scan duration 19 min 45 s) while maintaining high resolution with the combination of CS and SENSE.

2.3. Quantitative image analysis

Signal-to-noise ratio (SNR) and contrast-to-noise ratio (CNR) values were determined based on the subtraction method [12] for images acquired with SENSE only and with the combination of CS and SENSE. SNR was calculated for subchondral bone, joint fluid, cartilage, ligaments, muscle, fat and tendons. After acquiring the SNR for these structures, CNR was calculated for cartilage/fluid, subchondral bone/cartilage, ligaments/fluid and ligaments/fat. The sagittal sequences with SENSE only and with the combination of CS and SENSE were acquired twice in the same examination session and they were subtracted from each other in order to generate noise maps. Afterwards regions of interest (ROIs) were placed in identical locations on three consecutive central slices in each series as well as in the noise series. From the mean of these ROIs, SNR and CNR values were calculated following the formulas of previous methodologies using the subtraction method [12,13].

2.4. Semi-quantitative image analysis

Visual analysis of all sequences was performed with an integrated picture archiving and communication system (PACS) -viewing software. The semi-quantitative image analysis was performed by two musculoskeletal radiologists separately (J.N. and B.J.S.; 6 and 7 years of experience, respectively), blinded to clinical information and all other information. Grading of the depiction of anatomic structures was performed using an ordinal 5-point Likert scale (1 = poor, 2 = below average, 3 = fair, 4 = good, 5 = excellent), as previously performed [12]. The following criteria were evaluated with the grading of the image quality: partial volume effect, discrimination from adjacent tissues and anatomical structures as well as blurring. Moreover, the severity of motion artifacts was graded (1 = severe motion artifacts; 5 = no motion artifacts). In order to prevent a bias, the data sets with SENSE only and with the combination of CS and SENSE were assessed in a random order with an interval of four weeks. The following anatomical structures of the ankle were assessed and graded: the medial and lateral collateral ligament complex, the ligaments within the sinus tarsi (cervical ligament, interosseous talocalcaneal ligament), the tibiofibular syndesmosis, the extensor tendons, peroneal tendons and flexor tendons as well as articular cartilage and subchondral bone.

2.5. Statistical analysis

The data were analyzed using SPSS 25.0 (IBM, Armonk, N.Y., USA) (T.B. and B.J.S.). All statistical tests were performed two-sided using a level of significance (α) of 0.05 was used for all tests. The 2D sequences acquired with SENSE only are the current standard technique for MR imaging of the ankle and were therefore the standard of reference. Paired t-tests (for numeric variables) and McNemar's tests (for binary categorical variables) were used to evaluate differences in subject characteristics. Wilcoxon signed-rank test was used to evaluate differences regarding the image quality between sequences with SENSE only and with the combination of CS and SENSE. SNR and CNR between sequences acquired with SENSE only and with the combination of CS and SENSE were assessed with the Wilcoxon signed-rank test and were reported as mean values ± standard deviation. Cohen's κ was assessed for the agreement between the 2D TSE sequences with SENSE and with the combination of CS and SENSE for the pathologies found at the following anatomical structures of the ankles assessed: the medial and lateral collateral ligament complex, the ligaments within the sinus tarsi, the syndesmosis, the extensor tendons, peroneal tendons and flexor tendons as well as articular cartilage and subchondral bone. Fleiss' κ was used in order to determine the intra- and interreader agreement of MR imaging findings. For the intrareader agreement, two radiologists (initials blinded for review) repeated the readings of all patients once again after four weeks, blinded for previous results.

3. Results

3.1. Study subject characteristics and image quality

The 20 volunteers who underwent MR imaging with SENSE only and with the combination of CS and SENSE included 13 men and 7 women (mean age ± standard deviation, 30.2 ± 7.3 years). None of the MR images needed to be excluded due to severe motion artifacts. There was no statistically significant difference found between the 2D TSE sequences acquired withSENSE only and with the combination of CS and SENSE in the grading of the motion artifacts in the analyses performed by each reader (with SENSE versus with the combination of CS and SENSE: 4.8 ± 0.4 vs. 4.9 ± 0.3 and 4.7 ± 0.6 vs. 4.8 ± 0.4, P = 0.16-0.41, respectively).

3.2. Quantitative image analysis

There were no significant differences found in SNR between the 2D TSE sequences acquired with SENSE only and with the combination of CS and SENSE even though the SNR appeared to be higher on sequences with the combination of CS and SENSE (SNR with the combination of CS and SENSE compared to SNR with SENSE only: cartilage, 57.5 ± 37.4 vs. 41.0 ± 21.7; fluid, 71.5 ± 42.2 vs. 65.0 ± 32.2; muscle, 98.3 ± 68.3 vs. 56.8 ± 51.0; ligaments, 61.8 ± 74.6 vs. 25.0 ± 9.7; subchondral bone, 17.3 ± 5.7 vs. 19.8 ± 3.7; fat, 12.3 ± 6.2 vs. 46.5 ± 43.3; tendons, 21.2 ± 8.6 vs. 12.4 ± 8.4; P = 0.18-0.62; Fig. 1). Moreover, CNR of cartilage/fluid, subchondral bone/cartilage, ligaments/fluid and ligaments/fat did not differ significantly between the sequences acquired with SENSE only and with the combination of CS and SENSE ($P > 0.05$; Fig. 2).

3.3. Semi-quantitative image analysis

When comparing the anatomic structures of the lateral and medial collateral ligament complex, as well as the ligaments within the sinus tarsi and the syndesmosis (Table 2; Fig. 3) between sequences that were acquired with SENSE only and with the combination of CS and SENSE, all of these anatomic structures were considered to be equally depicted by all readers ($P > 0.05$). Moreover, there were no significant differences found between the sequences acquired with SENSE and with the combination of CS and SENSE in the depiction of the tibiofibular and talar cartilage (Fig. 4) as well as the tendons (Fig. 5) and the subchondral bone ($P > 0.05$; Table 3). One volunteer showed a osteochondral lesion at the medial shoulder of the talus that was detected on the sequences acquired with SENSE only and with the combination of CS and SENSE (Fig. 6) and a further volunteer showed thickening of the anterior talofibular ligament (Fig. 7). Two other volunteers showed cartilage lesions of their tibiofibular cartilage. The remaining 16 volunteers showed no abnormalities of their ankles in neither the sequences acquired with the combination of CS and SENSE nor in the sequences acquired with SENSE only, resulting in an agreement of κ = 1.00 in the assessment of pathologies of the ankles analyzed.

The inter-observer reliability was substantial for all criteria (κ = 0.75 - 0.89) and the intra-observer reliability was excellent (κ = 0.82 - 0.98), respectively.

4. Discussion

Our study has shown that using CS for the acquisition of 2D TSE MR imaging sequences of the ankle is feasible with a reduction in scan time of 20% without a significant decrease SNR, CNR or diagnostic

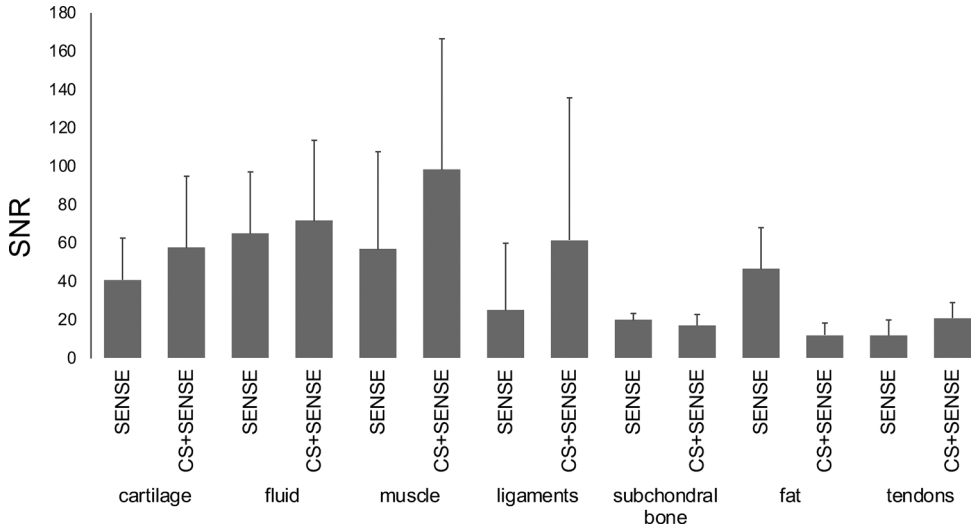

Fig. 1. SNR of the structures cartilage, fluid, muscle, ligaments, subchondral bone, fat and tendons. There was no significant difference found in SNR between the images acquired using SENSE only and the images acquired using the combination of CS and SENSE (CS + SENSE) ($P > 0.05$).

performance.

These findings are in line with previous anatomical musculoskeletal imaging studies. A previous study acquired a rapid 3D fast spin-echo sequence (CUBE) using compressed sensing at the knee and compared this sequence to a 3D CUBE without compressed sensing [4]. This previous study reported that a reduction the scan time by 30% was achieved for this 3D sequence while the diagnostic performance and SNR remained unchanged. Nevertheless, there was a significantly increased blurriness detected on the images acquired with compressed sensing when comparing these with sequences acquired without compressed sensing, which resulted in a decrease in clarity of cartilage, menisci, tendons as well as the muscle. Consequently, especially subtle joint pathologies could be missed in 3D sequences of the knee joint acquired with compressed sensing, unless the resolution is increased significantly compared to the resolution assessed in previous studies, which would cause the scan time to increase significantly and might therefore not become feasible. Moreover, other studies have demonstrated that in general 3D-TSE images of the joints showed increased blurring in comparison to 2D-FSE sequences [14–16].

A previous study used a three dimensional Gradient Recalled Acquisition in Steady State (GRASS) sequence in combination with compressed sensing for the evaluation of articular cartilage of the knee joints in pediatric patients [17]. This study considered compressed sensing to be feasible in a clinical setting, yet the study had focused on multiple different regions, such as the MR angiographies of the chest and the abdomen, and only eight patients with MR imaging of the knee were included in total. The same applies to Worters et al., who performed multispectral MR imaging of the spine to avoid MRI artifacts near metal, applying compressed sensing in order to reduce scan time [18]. Compressed sensing has also been applied in quantitative musculoskeletal imaging studies, such as the study performed by Pandit et al., who used a combination of parallel imaging and compressed sensing as well as a reconstruction algorithm in order to reduce the acquisition time of quantitative T1rho sequences for cartilage imaging [19]. In this previous study the scan time was reduced by 25% while there was no significant change regarding the assessed parameters.

To our knowledge, there is a lack of information on MR sequence performance with compressed sensing of the ankle in the literature. Our study demonstrated a reduction in scan time by 20% without a reduction of SNR. A reduction in scan time in about this range has been shown previously at the knee [4]. Yet, other previous studies reported on challenges regarding accurate measurement and assessment of

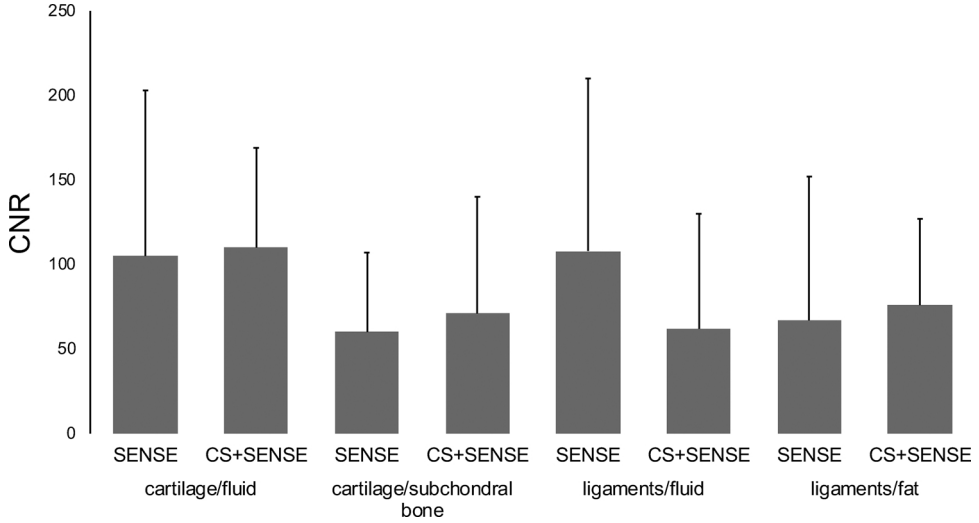

Fig. 2. CNR of cartilage/fluid, subchondral bone/cartilage, ligaments/fluid and ligaments/fat. There was no significant difference found in CNR between the images acquired using SENSE only and the images acquired using the combination of CS and SENSE (CS + SENSE) ($P > 0.05$).

Table 2
Comparison of the quality of depiction of ligamentous structures of the ankle of images acquired with sensitivity encoding (SENSE) only and with the combination of compressed sensing (CS) and SENSE (CS + SENSE)*.

	Reader 1		Reader 2	
	SENSE	CS + SENSE	SENSE	CS + SENSE
Lateral collateral ligament complex				
Anterior talofibular ligament	4.8 ± 0.4	4.9 ± 0.3	4.7 ± 0.4	4.8 ± 0.4
Calcaneofibular ligament	4.8 ± 0.4	4.9 ± 0.3	4.5 ± 0.5	4.7 ± 0.6
Posterior talofibular ligament	4.8 ± 0.4	4.9 ± 0.3	4.6 ± 0.5	4.7 ± 0.5
Medial collateral ligament complex				
Anterior tibiotalar ligament	4.8 ± 0.4	4.9 ± 0.3	4.5 ± 0.7	4.6 ± 0.5
Tibionavicular ligament	4.8 ± 0.4	4.9 ± 0.3	4.6 ± 0.5	4.6 ± 0.5
Tibiospring ligament	4.8 ± 0.4	4.9 ± 0.3	4.6 ± 0.5	4.7 ± 0.5
Calcaneotibial ligament	4.8 ± 0.4	4.9 ± 0.3	4.6 ± 0.5	4.7 ± 0.5
Posterior tibiotalar ligament	4.8 ± 0.4	4.9 ± 0.3	4.8 ± 0.4	4.9 ± 0.2
Ligaments within the sinus tarsi				
Cervical ligament	4.8 ± 0.4	4.9 ± 0.3	4.9 ± 0.3	4.8 ± 0.4
Interosseous talocalcaneal ligament	4.8 ± 0.4	4.9 ± 0.3	4.9 ± 0.3	4.8 ± 0.4
Syndesmosis				
Anterior tibiofibular ligament	4.8 ± 0.4	4.9 ± 0.3	4.8 ± 0.4	4.7 ± 0.5
Posterior tibiofibular ligament	4.8 ± 0.4	4.9 ± 0.3	4.6 ± 0.5	4.7 ± 0.5

5-point Likert scale (5 = best; 1 = worst).
$P < 0.05$.
* Data given as means ± standard deviations.

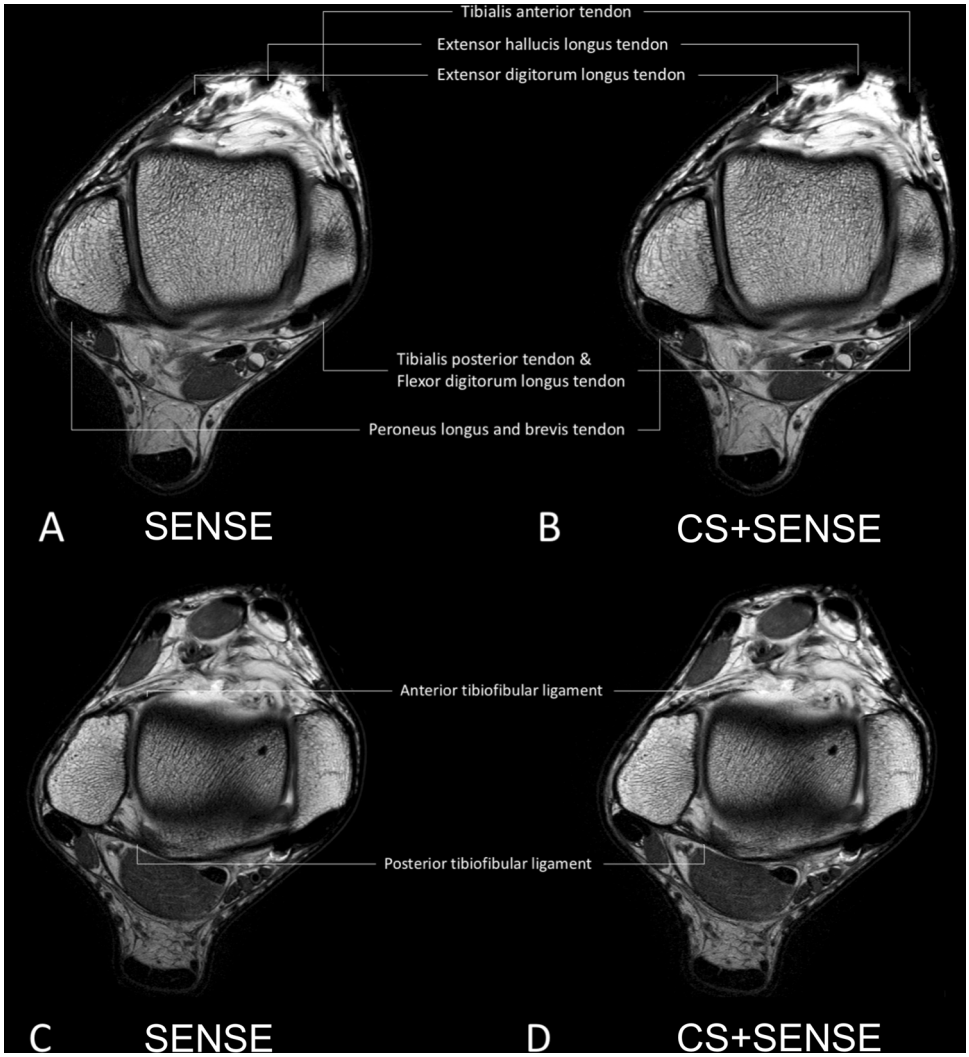

Fig. 3. Axial T2-weighted images acquired using SENSE only (A, C) and using the combination of CS and SENSE (CS + SENSE; B, D), illustrating the tendons as well as the syndesmosis assessed in the image analysis.

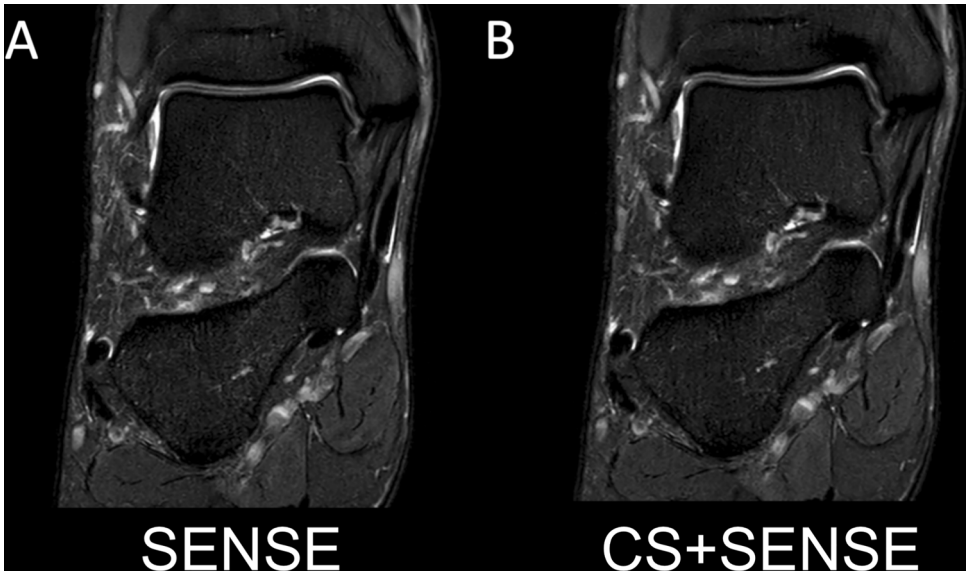

Fig. 4. Coronal IM-weighted images with fat saturation acquired using SENSE only (A) and using the combination of CS and SENSE (CS + SENSE; B). These images were useful for the depiction of the cartilage of the talocrural joint.

signal-to-noise ratio [20,21]. In our study, the measurements were performed using a double acquisition method in order to measure spatially variant noise [13,22]. Our results showed no significant differences regarding SNR and CNR in our study between the sequences acquired with compressed sensing and the sequences acquired with parallel imaging only.

It is worth to note that the employed combination of the CS and SENSE technique is a combination of compressed sensing and parallel imaging based on sensitivity encoding using the coil sensitivity information from calibration scans. Therefore, the employed combination of the CS and SENSE enables a smooth sampling density transition between the central and outer k-space parts. The employed method requires a reduced number of k-space samples at the central k-space region compared to compressed sensing methods requiring fully sampled k-space central regions. This ability to decrease the k-space sampling density around the k-space center is important in order to achieve an acceleration of up to 20% even in 2D imaging.

This study has limitations. A standard of reference such as arthroscopy was not available for our study and since this study was performed with volunteers, only very few study subjects included into this study showed pathologies at their ankle. Therefore, a comparison of ankle joint pathologies with an adequate standard of reference was not possible in our study. The small number of patients with pathologies needs to be noted as a limitation of this study and further studies

Table 3
Comparison of the quality of depiction of tendons, cartilaginous and bony structures of the ankle of images acquired with sensitivity encoding (SENSE) only and with the combination of compressed sensing (CS) and SENSE (CS + SENSE)*.

	Reader 1		Reader 2	
	SENSE	CS + SENSE	SENSE	CS + SENSE
Cartilage				
Tibiofibular cartilage	4.8 ± 0.6	4.8 ± 0.6	4.6 ± 0.5	4.9 ± 0.3
Talar cartilage	4.8 ± 0.6	4.8 ± 0.6	4.8 ± 0.4	4.9 ± 0.3
Tendons				
Extensor tendons	4.8 ± 0.5	5.0 ± 0.0	4.6 ± 0.6	4.3 ± 0.7
Peroneal tendons	4.8 ± 0.5	5.0 ± 0.0	4.7 ± 0.5	4.8 ± 0.4
Flexor tendons	4.8 ± 0.5	5.0 ± 0.0	4.7 ± 0.5	4.7 ± 0.5
Subchondral bone				
Talus	5.0 ± 0.0	4.9 ± 0.2	4.9 ± 0.4	4.9 ± 0.2
Fibula	5.0 ± 0.0	4.9 ± 0.2	4.9 ± 0.2	4.9 ± 0.2
Tibia	5.0 ± 0.0	4.9 ± 0.2	4.9 ± 0.2	4.8 ± 0.3

5-point Likert scale (5 = best; 1 = worst).
P < 0.05 written in bold.
* Data given as means ± standard deviations.

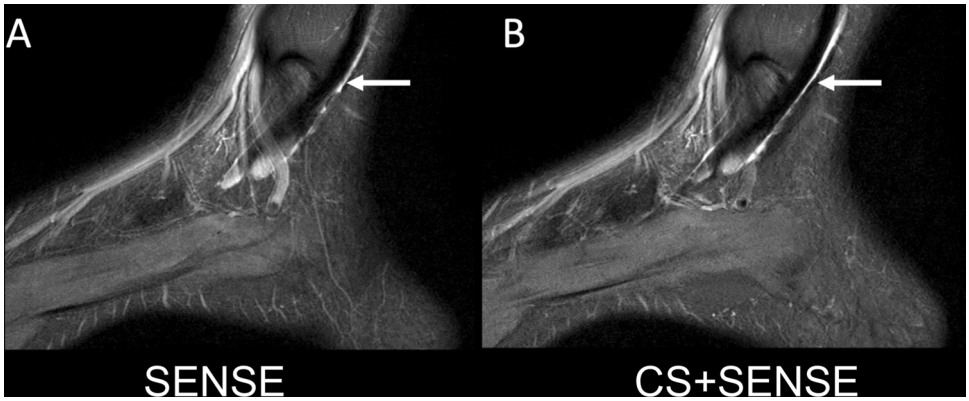

Fig. 5. Sagittal IM-weighted images with fat saturation acquired using SENSE only (A) and using the combination of CS and SENSE (CS + SENSE; B). The quality of the depiction of the flexor tendons (white arrows) were rated equally on both images by both readers.

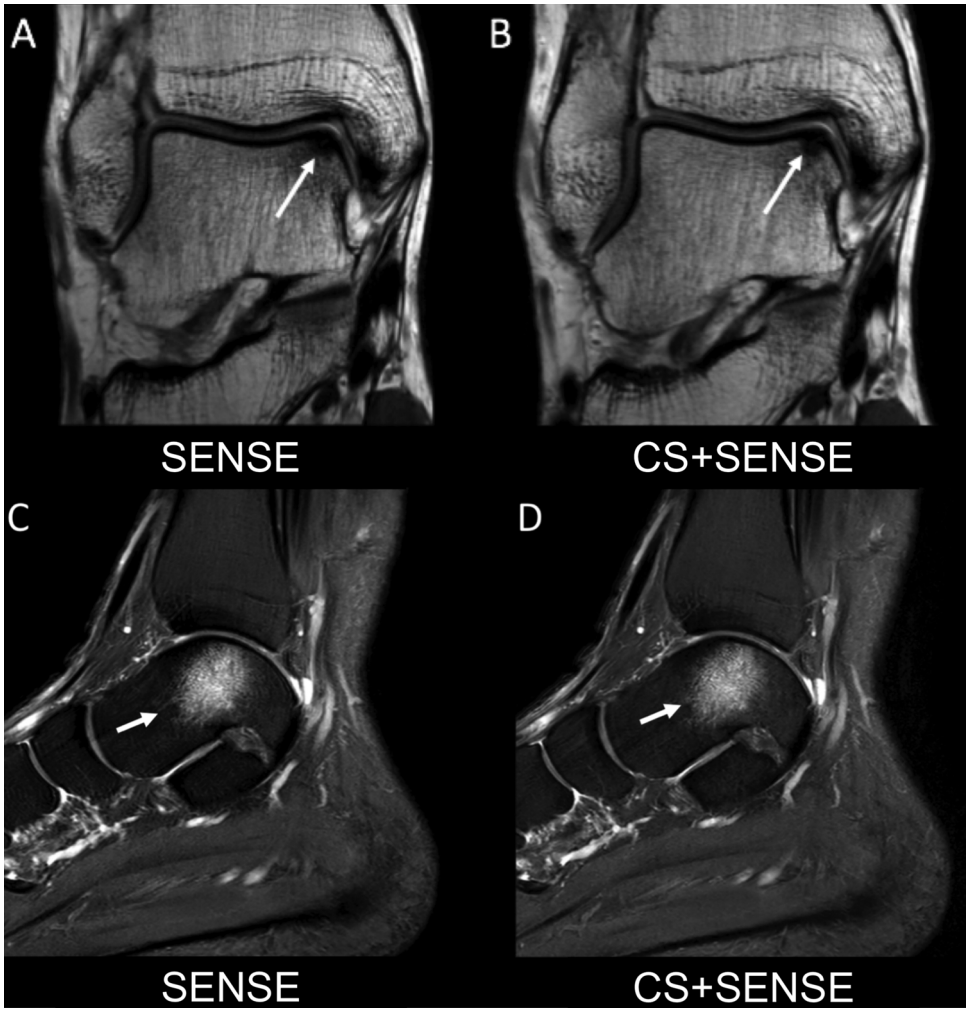

Fig. 6. Coronal T1-weighted images acquired using SENSE only (A) and using the combination of CS and SENSE (CS + SENSE; B) showing the ankle of a 42-year-old male volunteer with an osteochondral lesion (long white arrows). Sagittal IM-weighted images with fat saturation acquired with SENSE only (C) and using the combination of CS and SENSE (CS + SENSE; D) depicting bone marrow changes adjacent to the osteochondral lesion (short white arrows). The quality of the depiction of these findings was rated equally for the images acquired with SENSE only and with the combination of CS and SENSE.

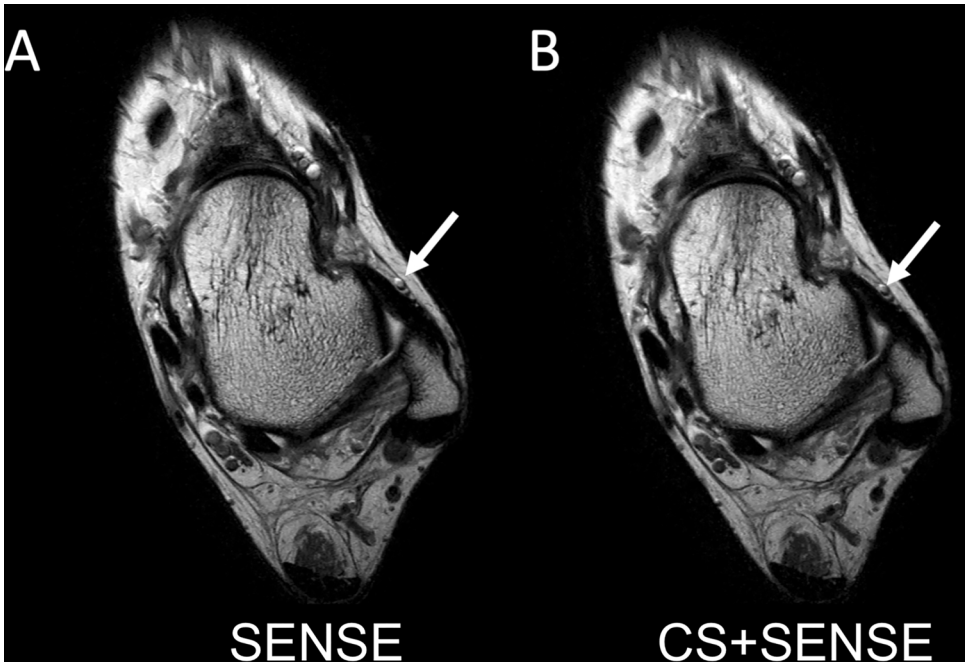

Fig. 7. Axial T2-weighted images acquired with SENSE only (A) and acquired with the combination of CS and SENSE (CS + SENSE; B) showing the ankle of a 28-year-old male volunteer with thickening of the anterior talofibular ligament (white arrows). The quality of the depiction of the ligaments were rated equally on both images by both readers.

evaluating both MR techniques in patients with specific pathologies at the ankle are needed in the future. An assessment in a larger cohort with following arthroscopy is therefore needed in order to validate our preliminary results. Moreover, the 2D-TSE sequence cannot be reformatted in multiple planes as for instance the 3D-FSE sequences. Nevertheless, the high resolution together with the image quality that can be achieved with 2D TSE sequences in reasonable scan time and is currently considered to be superior to the multi-plane reformats of 3D-TSE sequences.

5. Conclusion

Our study has shown that compressed sensing can provide a reduction in scan time of 20% when applied to 2D-TSE MR imaging of the ankle. Our study demonstrated that there was no decrease in the diagnostic performance, CNR or SNR when applying compressed sensing combined with SENSE to the acquisition of sequences in comparison to sequences acquired with SENSE only. Moreover, there was no image blurring detected as in previous studies assessing 3D joint imaging with compressed sensing. Additional studies with following arthroscopy as a standard of reference are needed in order to assess the diagnostic performance of these high-resolution sequences acquired with compressed sensing at the ankles of symptomatic patients.

References

[1] R.M. Gehrmann, S. Rajan, D.V. Patel, C. Bibbo, Athletes' ankle injuries: diagnosis and management, Am J Orthop (Belle Mead NJ) 34 (11) (2005) 551–561.

[2] Z.S. Rosenberg, J. Beltran, J.T. Bencardino, From the RSNA refresher courses. Radiological society of north America. MR imaging of the ankle and foot, Radiographics 20 (2000) S153–79 Spec No.

[3] B. Mengiardi, C.W. Pfirrmann, P. Vienne, J. Hodler, M. Zanetti, Medial collateral ligament complex of the ankle: MR appearance in asymptomatic subjects, Radiology 242 (3) (2007) 817–824.

[4] R. Kijowski, H. Rosas, A. Samsonov, K. King, R. Peters, F. Liu, Knee imaging: rapid three-dimensional fast spin-echo using compressed sensing, J. Magn. Reson. Imaging 45 (6) (2017) 1712–1722.

[5] R. Kijowski, K.W. Davis, M.A. Woods, M.J. Lindstrom, A.A. De Smet, G.E. Gold, R.F. Busse, Knee joint: comprehensive assessment with 3D isotropic resolution fast spin-echo MR imaging–diagnostic performance compared with that of conventional MR imaging at 3.0 T, Radiology 252 (2) (2009) 486–495.

[6] N. Subhas, A. Kao, M. Freire, J.M. Polster, N.A. Obuchowski, C.S. Winalski, MRI of the knee ligaments and menisci: comparison of isotropic-resolution 3D and conventional 2D fast spin-echo sequences at 3 T, AJR Am. J. Roentgenol. 197 (2) (2011) 442–450.

[7] H. Kudo, T. Inaoka, N. Kitamura, T. Nakatsuka, S. Kasuya, R. Kasai, M. Tozawa, K. Nakagawa, H. Terada, Clinical value of routine use of thin-section 3D MRI using 3D FSE sequences with a variable flip angle technique for internal derangements of the knee joint at 3T, Magn. Reson. Imaging 31 (8) (2013) 1309–1317.

[8] M. Lustig, D. Donoho, J.M. Pauly, Sparse MRI: the application of compressed sensing for rapid MR imaging, Magn. Reson. Med. 58 (6) (2007) 1182–1195.

[9] L. Feng, T. Benkert, K.T. Block, D.K. Sodickson, R. Otazo, H. Chandarana, Compressed sensing for body MRI, J. Magn. Reson. Imaging 45 (4) (2017) 966–987.

[10] S. Geethanath, R. Reddy, A.S. Konar, S. Imam, R. Sundaresan, R.B. DR, R. Venkatesan, Compressed sensing MRI: a review, Crit. Rev. Biomed. Eng. 41 (3) (2013) 183–204.

[11] O.N. Jaspan, R. Fleysher, M.L. Lipton, Compressed sensing MRI: a review of the clinical literature, Br. J. Radiol. 88 (1056) (2015) 20150487.

[12] M. Notohamiprodjo, B. Kuschel, A. Horng, D. Paul, P. Baer, G. Li, J.M. Garcia del Olmo, M.F. Reiser, C. Glaser, 3D-MRI of the ankle with optimized 3D-SPACE, Invest. Radiol. 47 (4) (2012) 231–239.

[13] O. Dietrich, J.G. Raya, S.B. Reeder, M.F. Reiser, S.O. Schoenberg, Measurement of signal-to-noise ratios in MR images: influence of multichannel coils, parallel imaging, and reconstruction filters, J. Magn. Reson. Imaging 26 (2) (2007) 375–385.

[14] K.J. Stevens, R.F. Busse, E. Han, A.C. Brau, P.J. Beatty, C.F. Beaulieu, G.E. Gold, Ankle: isotropic MR imaging with 3D-FSE-cube–initial experience in healthy volunteers, Radiology 249 (3) (2008) 1026–1033.

[15] K.J. Stevens, C.G. Wallace, W. Chen, J.K. Rosenberg, G.E. Gold, Imaging of the wrist at 1.5 Tesla using isotropic three-dimensional fast spin echo cube, J. Magn. Reson. Imaging 33 (4) (2011) 908–915.

[16] O. Ristow, C. Stehling, R. Krug, L. Steinbach, G. Sabo, A. Ambekar, M. Huber, T.M. Link, Isotropic 3-dimensional fast spin echo imaging versus standard 2-dimensional imaging at 3.0 T of the knee: artificial cartilage and meniscal lesions in a porcine model, J. Comput. Assist. Tomogr. 34 (2) (2010) 260–269.

[17] S.S. Vasanawala, M.T. Alley, B.A. Hargreaves, R.A. Barth, J.M. Pauly, M. Lustig, Improved pediatric MR imaging with compressed sensing, Radiology 256 (2) (2010) 607–616.

[18] P.W. Worters, K. Sung, K.J. Stevens, K.M. Koch, B.A. Hargreaves, Compressed-sensing multispectral imaging of the postoperative spine, J. Magn. Reson. Imaging 37 (1) (2013) 243–248.

[19] P. Pandit, J. Rivoire, K. King, X. Li, Accelerated T1rho acquisition for knee cartilage quantification using compressed sensing and data-driven parallel imaging: a feasibility study, Magn. Reson. Med. 75 (3) (2016) 1256–1261.

[20] Y. Ding, L. Ying, N. Zhang, D. Liang, Noise behavior of MR brain reconstructions using compressed sensing, Conf. Proc. IEEE Eng. Med. Biol. Soc. (2013) 5155–5158 2013.

[21] Y. Ding, Y.C. Chung, O.P. Simonetti, A method to assess spatially variant noise in dynamic MR image series, Magn. Reson. Med. 63 (3) (2010) 782–789.

[22] S.B. Reeder, B.J. Wintersperger, O. Dietrich, T. Lanz, A. Greiser, M.F. Reiser, G.M. Glazer, S.O. Schoenberg, Practical approaches to the evaluation of signal-to-noise ratio performance with parallel imaging: application with cardiac imaging and a 32-channel cardiac coil, Magn. Reson. Med. 54 (3) (2005) 748–754.